

# 18 CM OBSERVATIONS OF GALACTIC OH FROM LONGITUDES 128° TO 300°

By R. N. MANCHESTER,\*† B. J. ROBINSON,\* and W. M. GOSS\*

[Manuscript received May 5, 1970]

## Abstract

Observations have been made of 18 cm OH emission and/or absorption for 12 sources between galactic longitudes 128° and 300°. The OH is seen in emission in five of the sources, and the four Stokes parameters of the emission profiles have been measured. A new type of strong wideband OH emission has been found near  $l^{\text{II}} = 284^\circ$ . There are two sources where weak emission at 1612 MHz accompanies absorption on the other three lines. The relationship of the OH to nearby HII regions has been investigated by position measurements and by a comparison of OH and recombination line radial velocities.

## I. INTRODUCTION

Observations are presented of the four ground-state transitions of the OH molecule associated with 12 sources in the galactic longitude range 128°–300°. This is the third paper in a series dealing with 18 cm OH observations carried out with the 210 ft telescope at Parkes. The first paper (Robinson, Goss, and Manchester 1970) dealt with instrumentation and other details common to all observations, and gave results for sources in the longitude range 350°–50°. In the second paper (Goss, Manchester, and Robinson 1970) sources in the longitude range 305°–334° were discussed.

Absorption at 1665 or 1667 MHz had been previously detected in five of the sources by McGee, Gardner, and Robinson (1967). In two of these sources we find OH emission at 1612 MHz and absorption at 1665, 1667, and 1720 MHz. Three OH emission sources and one absorption source have been found during a survey at 1665 MHz of the region between  $l^{\text{II}} = 284^\circ$  and 300°. The strong broad emission found in G284.2–0.8 at 1612 and 1665 MHz has been reported previously by Manchester, Goss, and Robinson (1969*a*, 1969*b*). We have also made further observations of the three sources CIT–3 (Wilson and Barrett 1968), W 12 (Goss 1968), and Orion A. An upper limit has been set to any Zeeman splitting of the W 12 absorption profile.

## II. INSTRUMENTATION

The equipment and methods of observation have been described by Robinson, Goss, and Manchester (1970). A bandwidth of 1 kHz was used for the emission profiles, which were recorded with right-hand (R.H.) and left-hand (L.H.) circular polarization and with the linear Stokes parameters  $Q$  and  $U$ . A bandwidth of 10 kHz was used for the absorption profiles and for spectra taken at the continuum maxima of the emission sources.

\* Division of Radiophysics, CSIRO, P.O. Box 76, Epping, N.S.W. 2121.

† Present address: National Radio Astronomy Observatory, Charlottesville, Virginia, U.S.A.

## III. SUMMARY OF OBSERVATIONS

Properties of the continuum sources associated with the OH emission or absorption discussed in this paper are given in Table 1. As in the previous papers in this series, the galactic G numbers are from the 6 cm survey of Goss and Shaver (1970), and the radial velocities and kinematic distances of the sources are from the hydrogen  $109\alpha$  recombination line survey of Wilson *et al.* (1970). The equatorial coordinates and antenna temperature refer to the continuum maximum of the source found with a 12' arc beam at 18 cm wavelength.

TABLE 1  
PROPERTIES OF BACKGROUND SOURCES

Galactic Source Number	Previous Designation	18 cm Position (1950)				Continuum Spectrum	H109 $\alpha$ Velocity (km sec <sup>-1</sup> )	Kinematic Distance (kpc)	$T_a$ at 18 cm (°K)
		R.A.		Dec.					
		h	m	s	°				
G128.6-50.1	CIT-3	01	03	46	+12 19.5	I.R. object			
G206.5-16.4	W 12	05	39	12	-01 55.5	Thermal	+6.6	0.6	36
G209.0-19.4	Orion A	05	32	47	-05 24.7*	Thermal	-2.2	0.5	190
G265.1+1.5	RCW 36	08	57	34	-43 32.2	Thermal	+3.4	0.6 (1.5)	16
G267.9-1.1	RCW 38	08	57	18	-47 19.7	Thermal	+2.4	0.6 (1.5)	95
G282.0-1.2		10	04	55	-56 56.4	Thermal	+23.0	7.0	23
G284.0-0.9	RCW 48	10	17	35	-57 46.4	Thermal	+5.1	4.0	18
G284.3-0.3	RCW 49	10	22	27	-57 31.1	Thermal	-0.1	6.0	116
G285.3-0.0		10	29	48	-57 46.7	Thermal	-1.0	5.3	12
G287.5-0.6	Carina Neb.	10	42	12	-59 22.6	Thermal	{ -17.5 -23.0	2.7	98
G291.3-0.7	NGC 3576	11	09	50	-61 01.7	Thermal	-22.8	3.6	49
G291.6-0.5	NGC 3603	11	13	15	-60 58.5	Thermal	+10.4	8.4	110

\* OH emission position.

TABLE 2  
POSITIONS OF EMISSION SOURCES

Galactic Source Number	Previous Designation	OH Position (1950)				18 cm $T_a$ at OH Position (°K)	Lines Used for Position (MHz)
		R.A.		Dec.			
		h	m	s	°		
G128.6-50.1	CIT-3	01	03	46±4*	12 19.9±1*	—	1612
G209.0-19.4	Orion A	05	32	47†	-05 24.7†	190	1665
G284.2-0.8	RCW 48	10	19	42±8	-57 50.1±1	5	1612, 1665
G285.2-0.0		10	29	31±16	-57 45.3±2	11	1665
G291.6-0.4	NGC 3603	11	13	00±24	-60 54.5±3	80	1665

\* This is the position for the 27 km sec<sup>-1</sup> feature. In addition, the position R.A. 01<sup>h</sup> 03<sup>m</sup> 48<sup>s</sup> ± 4<sup>s</sup>, Dec. 12° 19' 7 ± 1' was determined for the -9.5 km sec<sup>-1</sup> feature. The position of the optical object is R.A. 01<sup>h</sup> 03<sup>m</sup> 46<sup>s</sup>, Dec. 12° 19' 5 (epoch 1950).

† Position taken from McGee, Gardner, and Robinson (1967). Raimond and Eliasson (1969) give R.A. 05<sup>h</sup> 32<sup>m</sup> 46<sup>s</sup>.9 ± 0<sup>s</sup>.2, Dec. -05° 24' 18" ± 3" for the features in the 17.6-23.7 km sec<sup>-1</sup> range.

For the 1665 MHz survey of the region  $284^\circ \leq \mu \leq 300^\circ$  observations were made at the continuum maximum of each source having an antenna temperature greater than 15°K on the 20 cm galactic map of Hill (1968). The survey profiles were in most cases taken with R.H. circular polarization and 10 kHz resolution. No OH emission or absorption, with a limit of 1°K in antenna temperature, was observed in the following sources: G286.2-0.2, 289.1-0.4, 289.8-1.1, 290.1-0.8, 291.0-0.1, 292.0+1.8, 295.0-1.7, 295.2-0.6, 298.2-0.3, and 298.9-0.4.

The positions for the OH emission were determined by means of observations at a grid of points spaced at half-beamwidth (6' arc) intervals; these are given in Table 2. The transition used for the position measurement is noted in each case and each source has been assigned a galactic coordinate catalogue number. None of the emission sources could be resolved with the 12' arc beam. The 18 cm continuum

TABLE 3  
POLARIZATION OF EMISSION FEATURES  
Errors are based on peak-to-peak noise of R.H., L.H.,  $Q$ , and  $U$  measurements

Source	Line Frequency (MHz)	Radial Velocity (km sec <sup>-1</sup> )	Peak Flux Density (f.u.)	Line Width (km sec <sup>-1</sup> )	Circular Polarization* (%)	Linear Polarization† (%)	Position Angle (deg)	Axial Ratio*
G128.6-50.1	1612	-9.5	19±2	1.0	<12	<9		
	1612	26.8	17±2	1.0	<13	<8		
G209.0-19.4	1612	7.2	6±3	0.3	<45	a		
	1612	7.7	7±3	0.5	100±50	a		
	1665	-5.7	12±2	0.4	70±20	<15		1.0 ±0.2
	1665	3.3	11±2	0.4	-30±20	<14		-1.0 ±0.5
	1665	4.3	16±2	0.5	100±20	<10		1.0 ±0.1
	1665	6.2	7±2	0.6	95±45	<24		1.0 ±0.3
	1665	7.3	18±2	1.1	b	<14		
	1665	16.5	5±2	1.6	b	<30		
	1665	19.0	8±2	2.1	60±30	<20		1.0 ±0.3
	1665	20.7	17±2	1.2	<13	<10		
1665	22.8	20±2	1.2	b	<10			
G284.2-0.8	1612	-33.1	8±2	1.0	<25	a		
	1612	-24.5	91±2	14.0	<4	<2		
	1665	-27.5	80±2	0.3	5±3	15±3	90±5	0.15±0.1
	1665	-27.0	110±2	0.3	-10±3	10±3	125±10	0.5 ±0.2
	1665	-26.0	80±2	1.2	16±3	3±2	0±45	
	1665	-21.0	60±2	8.0	<4	<2		
	1665	-16.0	17±2	1.0	-60±5	<5		
	1665	-12.5	13±2	3.0	<30	<10		
	1665	14.0	13±1	3.0	<10	a, c		
G285.2-0.0	1665	4.2	14±3	0.5	-100±35	<20		
	1665	5.7	12±3	0.7	100±35	<20		
	1665	8.7	6±3	0.5	-90±65	<25		
G291.6-0.4	1665	14.6	8±3	0.3	-100±50	<20		
	1665	18.0	4±3	0.6	85±75	<35		

\* Negative sign indicates R.H. circular polarization; b indicates irregular change of circular polarization across this component.

† a indicates no linear polarization data; c indicates data from profiles with 10 kHz resolution.

temperatures at the OH positions are also given. Polarization information for all emission lines is presented in Table 3. Errors have been calculated using the peak-to-peak noise on the profiles.

In Table 4 the parameters of the absorption profiles, taken in each case at the source continuum maximum, are listed. The various quantities in the table are as defined by Robinson, Goss, and Manchester (1970). For G291.3-0.7 and G291.6-0.4 profiles were taken over a grid of points on the continuum sources; this is discussed in more detail in Section IV(*k*).

TABLE 4  
ABSORPTION LINE DATA

Source	Line Frequency (MHz)	Radial Velocity (km sec <sup>-1</sup> )	Absorption Depth (°K)	Optical Depth $\tau_m$	Line Width $\Delta V$ (km sec <sup>-1</sup> )	$N_{OH}/T_s$ ( $10^{14}$ cm <sup>-2</sup> degK <sup>-1</sup> )	Kinematic Distance (kpc)	Notes*
G206.5-16.4	1612	9.32 ± 0.14	1.6 ± 0.6	0.042 ± 0.017	1.2 ± 0.4			
	1665	9.57 ± 0.10	6.8 ± 1.3	0.21 ± 0.04	1.4 ± 0.2			
	1667	9.33 ± 0.04	9.4 ± 0.8	0.31 ± 0.02	1.5 ± 0.1	1.09 ± 0.05	1.0	a
	1667	12.48 ± 0.04	0.8 ± 0.3	0.03 ± 0.01	1.4 ± 0.1	0.10 ± 0.03		a
	1720	9.51 ± 0.15	2.3 ± 0.5	0.062 ± 0.014	1.9 ± 0.4			
	1665	5.2 ± 0.5	1.2 ± 0.4	0.08 ± 0.025	4.9 ± 1.3			
G265.1+1.5	1667	5.7 ± 0.3	2.3 ± 0.5	0.15 ± 0.03	3.8 ± 0.7			
	1720	6.1 ± 0.7	1.0 ± 0.5	0.08 ± 0.03	3.7 ± 1.8	1.44 ± 0.18	1.4	
	1612	0.1 ± 0.4	1.1 ± 0.4	0.015 ± 0.004	4.8 ± 0.9			
	1665	1.56 ± 0.18	9.6 ± 0.8	0.10 ± 0.01	5.9 ± 0.4			
G267.9-1.1	1667	1.84 ± 0.14	14.8 ± 1.0	0.16 ± 0.01	6.1 ± 0.4		0.86	
	1720	2.1 ± 0.3	4.9 ± 0.7	0.054 ± 0.007	5.6 ± 0.7	2.30 ± 0.09		
	1612	-8.6 ± 1.5	0.5 ± 0.4	0.023 ± 0.02	5.0 ± 3.5			
	1665	-4.8 ± 1.1	0.75 ± 0.3	0.033 ± 0.013	7.7 ± 2.5			
G284.3-0.3	1667	-4.3 ± 1.2	1.2 ± 0.5	0.055 ± 0.022	9.5 ± 2.9	1.3 ± 0.3	1.0 or 3.1	
	1667	-13.1 ± 0.8	1.5 ± 0.6	0.014 ± 0.006	6.1 ± 1.8	0.22 ± 0.06	2.5	b
	1667	0.2 ± 0.8	0.6 ± 0.16	0.005 ± 0.002	14.2 ± 1.8	0.17 ± 0.04	5.0	
	1665	-25.9 ± 1.1	1.2 ± 0.7	0.014 ± 0.007	5.2 ± 2.5			
G287.5-0.6	1667	-25.0 ± 1.1	1.2 ± 0.5	0.014 ± 0.005	8.3 ± 2.5	0.25 ± 0.07	3.0	b
	1612	-26.5 ± 0.4	2.1 ± 0.5	0.047 ± 0.010	4.0 ± 0.9			
	1665	-25.9 ± 0.3	6.6 ± 1.0	0.150 ± 0.020	5.1 ± 0.6			
	1667	-25.8 ± 0.2	7.9 ± 1.0	0.174 ± 0.022	4.7 ± 0.4	1.93 ± 0.02	3.6	b
G291.3-0.7	1720	-24.8 ± 0.5	1.2 ± 0.5	0.028 ± 0.010	2.7 ± 1.1			
	1612	12.1 ± 0.6	1.1 ± 0.8	0.010 ± 0.007	2.7 ± 1.6			c
	1665	12.0 ± 2.0	1.5 ± 1.4	0.014 ± 0.013	6.3 ± 4.4			d
	1667	13.1 ± 1.3	1.3 ± 1.1	0.013 ± 0.010	4.3 ± 2.8	0.13 ± 0.07	8.6	

\* Notes: a, kinematic distance greater than source distance; b, OH near tangential point; c, optical depth and line width uncorrected for bandwidth; d, emission adjacent to absorption line.

For those cases where significant absorption was observed at more than one frequency the relative intensities of the lines are compared in Table 5 by taking the ratio of the integrated areas of the absorption profiles. When the optical depth is small the ratios for 1612 : 1665 : 1667 : 1720 MHz would be 1 : 5 : 9 : 1 if the molecular levels were in thermal equilibrium. As Goss (1968) found for northern sources, the relative intensities at 1665 and 1667 MHz are frequently close to the expected ratio

TABLE 5  
RATIOS OF INTEGRATED AREAS OF ABSORPTION LINES

Source	1667 MHz Radial Velocity (km sec <sup>-1</sup> )	Frequency Ratio (MHz)	Ratio of Integrated Areas*	Implied 1667 MHz Optical Depth	Expected Ratio for Satellites from 1667 : 1665 Ratio
G206.5-16.4	9.3	1667 : 1612	8.9 ± 2.4	0.2	4.5
		1667 : 1665	1.43 ± 0.2	1.9	—
		1667 : 1720	3.4 ± 0.5	4.6	4.5
G265.1+1.5	5.7	1667 : 1612	E	—	6.2
		1667 : 1665	1.59 ± 0.38	0.9	—
		1667 : 1720	2.24 ± 0.75	10.3	6.2
G267.9-1.1	1.8	1667 : 1612	E	—	6.0
		1667 : 1665	1.55 ± 0.11	1.1	—
		1667 : 1720	3.21 ± 0.34	5.1	6.0
G282.0-1.2	-4.3	1667 : 1612	4.6 ± 2.9	3.3	9.0
		1667 : 1665	2.1 ± 0.8	0	—
		1667 : 1720	≥ 6.0	—	9.0
G284.3-0.3	-13.1	1667 : 1612	11.8 ± 3.2	0	9
		1667 : 1665	2.7 ± 0.6	0	—
		1667 : 1720	5.7 ± 1.7	1.2	9
G287.5-0.6	-25.0	1667 : 1612	> 5	—	5.1
		1667 : 1665	1.5 ± 0.7	1.5	—
		1667 : 1720	> 10	—	5.1
G291.3-0.7	-25.8	1667 : 1612	4.5 ± 0.8	3.5	1.19
		1667 : 1665	1.11 ± 0.14	16.7	—
		1667 : 1720	10.7 ± 3.2	0	1.19

\* E indicates that 1612 MHz appears in emission.

of 1.8; the most notable exception here is G291.3-0.7. The optical depth for the 1667 MHz line corresponding to each line ratio has been computed, assuming that the excitation temperature is the same for the two transitions. The 1667 : 1612 and 1667 : 1720 MHz ratios are very different from those expected from the 1667 : 1665 ratio and are usually unequal. In the case of RCW 38, and probably RCW 36, the 1612 MHz line appears in emission while 1720 MHz is in absorption.

#### IV. DISCUSSION OF INDIVIDUAL SOURCES

##### (a) G128.6-50.1

The OH source G128.6-50.1 is a 1612 MHz emission region found by Wilson and Barrett (1968) to be associated with the infrared star CIT-3. These authors

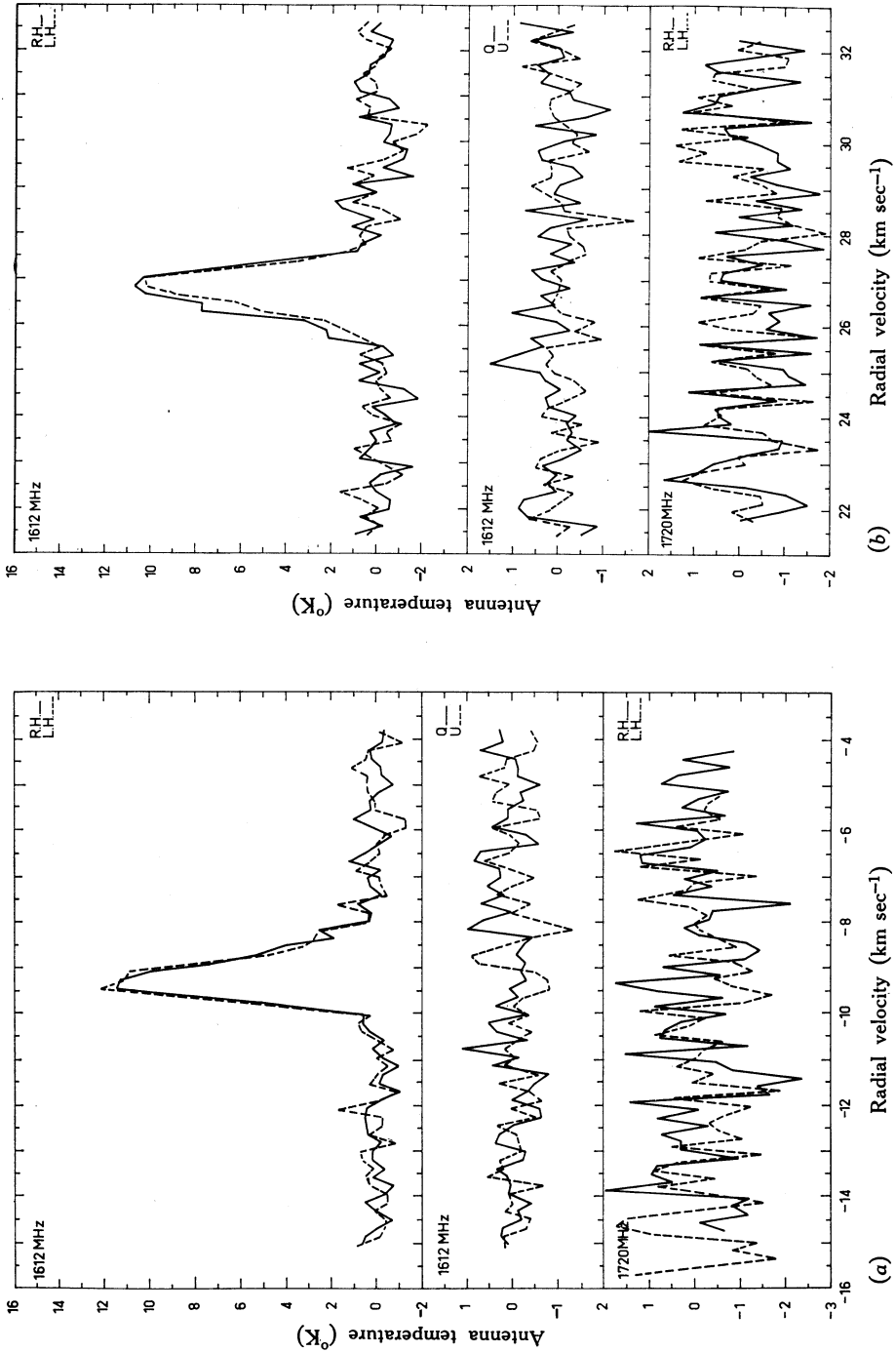


Fig. 1.—Observations of the infrared star CIT -3 at 1612 and 1720 MHz for the radial velocity ranges (relative to the local standard of rest) of (a) -15 to -4 km sec<sup>-1</sup> and (b) +22 to +32 km sec<sup>-1</sup>. The polarization of the OH emission is represented by R.H. and L.H. circular polarization and the linear Stokes parameters Q and U. The filter bandwidth is 1 kHz.

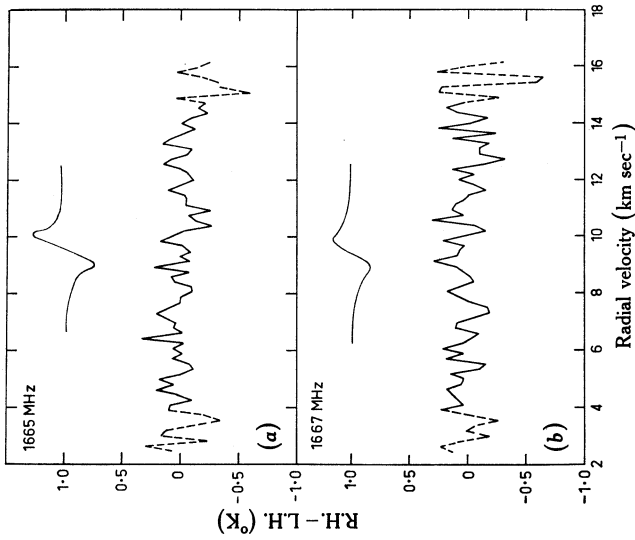
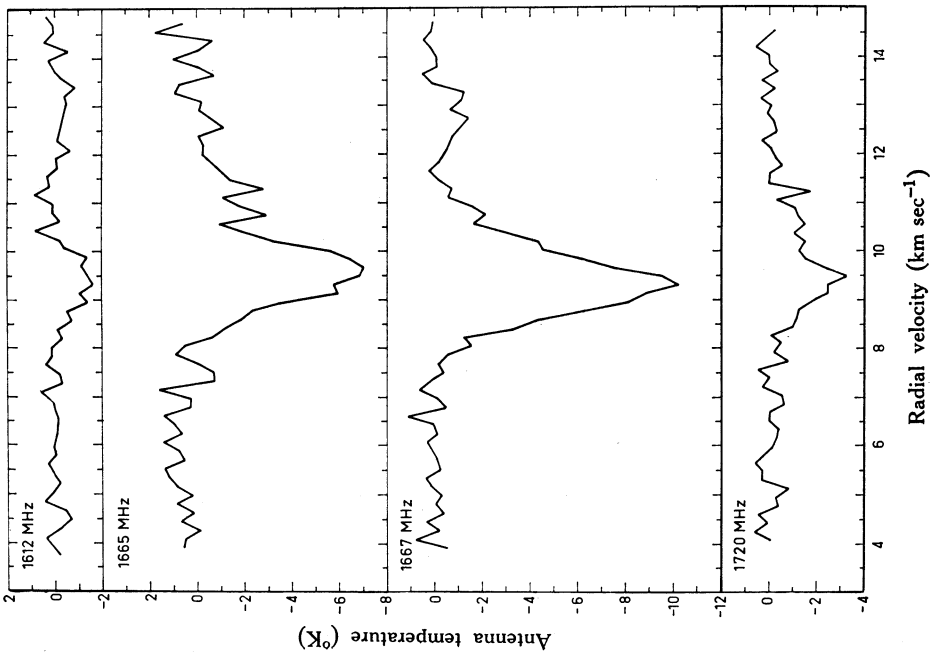


Fig. 2 (left).—OH absorption of W12 (G206.5-16.4). The bandwidth is 1 kHz.

Fig. 3 (above).—Measurements of the Stokes parameter  $-V$  for W12 at (a) 1665 MHz and (b) 1667 MHz. The integration times were 10.5 hr for (a) and 8.5 hr for (b); the dashed sections of the profiles had shorter integration times. The bandwidth is 1 kHz for both profiles. Displaced above the measurements are the expected Zeeman patterns for a longitudinal magnetic field of  $5 \times 10^{-5}$  G.



showed that the 1612 MHz emission is concentrated in two velocity groups near  $-9.5 \text{ km sec}^{-1}$  and  $+27 \text{ km sec}^{-1}$ , but found no emission at 1665 or 1720 MHz and only weak emission at 1667 MHz. Here we have only studied the 1612 and 1720 MHz profiles.

The positional information is summarized in Table 2; in agreement with Wilson and Barrett (1968), we find that both the  $-9.5$  and  $+27 \text{ km sec}^{-1}$  components arise from the same position, coincident with the infrared star. The 1612 and 1720 MHz profiles are shown in Figures 1(a) ( $-9.5 \text{ km sec}^{-1}$  feature) and 1(b) ( $+27 \text{ km sec}^{-1}$  feature). The polarization properties are summarized in Table 3. There is remarkable similarity between the two features; to within the noise the peak flux, width, and polarization of the two features are identical. No 1720 MHz emission greater than  $2^\circ\text{K}$  antenna temperature could be detected.

(b) *G206.5-16.4*

The radio source G206.5-16.4 or W 12 is the well-known HII region NGC 2024 situated at a distance of 0.6 kpc. The OH absorption lines in W 12, discovered by Goss (1968), have the largest optical depths found to date outside of the galactic centre. The four ground-state OH profiles are shown in Figure 2 (1 kHz resolution). The suggestion made by Goss (1968) that the 1720 MHz line is stronger than the 1612 MHz line is confirmed in the present investigation; the ratio of the mean intensities is about 1.5. In addition to the line at  $9.3 \text{ km sec}^{-1}$ , a weaker line is seen on the 1667 MHz profile at  $12.5 \text{ km sec}^{-1}$ . This feature is also evident on the 1667 MHz profile published by Goss (1968).

The properties of the absorption lines are summarized in Table 4 and the ratios of the integrated areas of the profiles are listed in Table 5. The velocity of the OH agrees very closely with a strong HI absorption at  $9.7 \text{ km sec}^{-1}$  observed by Radhakrishnan (personal communication). The measured optical depth for the 1667 MHz line is nearly twice as large as the next strongest absorption found in this survey, the 1667 MHz absorption of G291.3-0.7, which has a line width three times greater than for W 12. The relative intensities of the four lines indicate that a single excitation temperature cannot describe the population distribution.

The W 12 absorption profile is the narrowest OH absorption feature known and has a high optical depth. It is therefore most suitable for a measurement of Zeeman splitting of the absorption profile. Figure 3(a) shows measurements of the Stokes parameter  $V$  (L.H.—R.H. circular polarization) at 1665 MHz. Displaced above the  $V$  profile is the expected Zeeman pattern for a longitudinal magnetic field of  $5 \times 10^{-5} \text{ G}$ , obtained by differentiating the absorption profile in Figure 2. Figure 3(b) shows similar measurements at 1667 MHz. It is clear that the magnetic field strength in the absorbing OH clouds is less than  $5 \times 10^{-5} \text{ G}$ .

(c) *Orion A*

The OH spectrum in the direction of Orion A has been discussed in detail by Palmer and Zuckerman (1967), Goss (1968), and Weaver, Dieter, and Williams (1968). In Figure 4 the 1612 and 1665 MHz profiles are shown; the polarization parameters are given in Table 3.

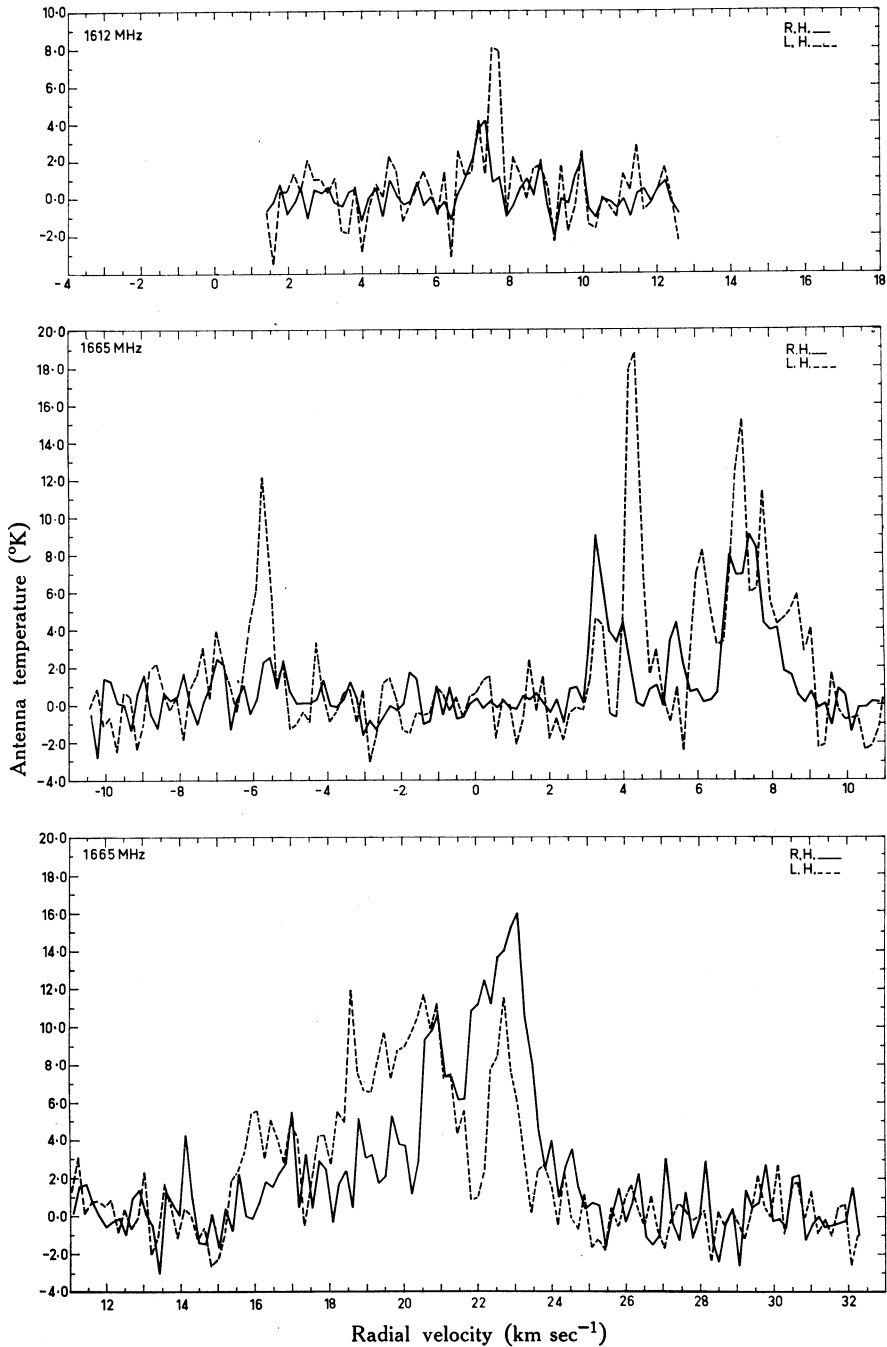


Fig. 4.—Polarization of the OH emission from Orion A. The 1612 MHz profile was recorded in April 1968 and the 1665 MHz profile in December 1967. The bandwidth is 1 kHz.

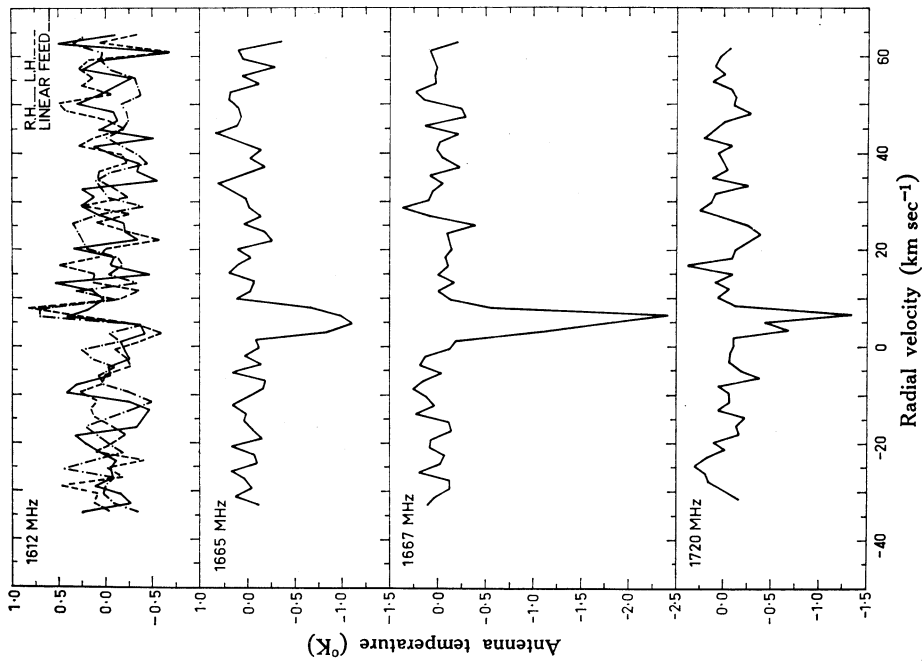


Fig. 5.—OH profiles for RCW 36 (G265.1+1.5). The absorption profiles at 1665, 1667, and 1720 MHz are averages of measurements with R.H. and L.H. circular polarization. The bandwidth is 10 kHz.

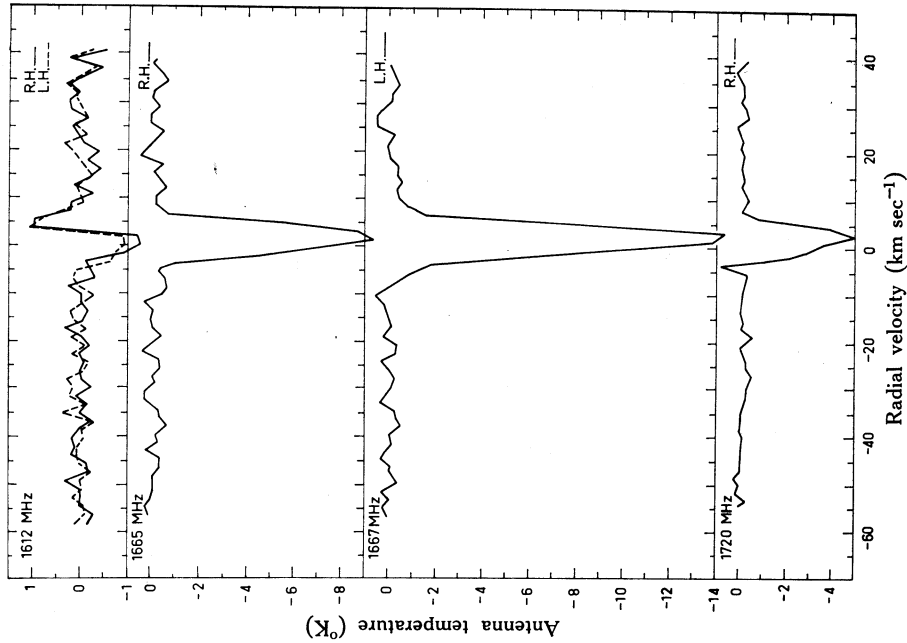


Fig. 6.—OH profiles for RCW 38 (G267.9-1.1). The absorption profiles at 1665, 1667, and 1720 MHz are averages of measurements with R.H. and L.H. circular polarization. The bandwidth is 10 kHz.

*(d) G265.1+1.5*

The continuum source G265.1+1.5 is the HII region RCW36 (Rodgers, Campbell, and Whiteoak 1960), which has been mapped at 2700 MHz by Manchester and Goss (1969). 1665 MHz OH absorption was first detected by McGee, Gardner, and Robinson (1967). Observations of the H109 $\alpha$  recombination line indicate that the distance to RCW36 is between 0.6 and 1.5 kpc.

The four OH ground-state profiles in Figure 5 show absorption on all transitions except 1612 MHz. It is probable that there is a weak emission line on the 1612 MHz profile at +7 km sec<sup>-1</sup>, very close to the absorption velocity on the other frequencies; this line may be L.H. polarized. We have no positional information on this emission.

The properties of the absorption lines are summarized in Tables 4 and 5. The OH absorption velocity of 5.7 km sec<sup>-1</sup> is close to an HI absorption line at 4.8 km sec<sup>-1</sup> detected by Radhakrishnan (personal communication); Goss, Murray, and Radhakrishnan (1970) give a lower limit to the distance of 1.3 kpc.

*(e) G267.9-1.1*

The radio source G267.9-1.1, one of the strongest southern galactic sources, is the well-known HII region RCW38. The area of RCW38 has been mapped by Manchester and Goss (1969). Absorption at 1665, 1667, and 1720 MHz was originally observed by McGee *et al.* (1965). Figure 6 shows the four ground-state OH profiles taken with 10 kHz resolution. Absorption is found on all four lines; in addition an emission line is observed at 1612 MHz. The properties of the absorption lines are summarized in Table 4 and the line ratios are given in Table 5. The total velocity range for each of the four lines is approximately the same. However, at 1612 MHz the higher velocity portion of the line appears in emission; this is centred at  $4.0 \pm 0.2$  km sec<sup>-1</sup> and has no detectable circular polarization. At present we have no positional information on the emission. The structure of the 1612 MHz profile is quite similar to the 1720 MHz line in the zero-velocity feature of Cas A (Rogers and Barrett 1967; Goss 1968).

Clark, Radhakrishnan, and Wilson (1962) found that RCW38 shows strong 21 cm absorption. Radhakrishnan (personal communication) finds at least two deep 21 cm absorption lines in the direction of RCW38: one at 2.3 km sec<sup>-1</sup> and another sharper line at 7.0 km sec<sup>-1</sup>. The OH absorption at about 2 km sec<sup>-1</sup> is probably associated with the broader hydrogen absorption centred at 2.3 km sec<sup>-1</sup>. The velocity of the OH absorption is close to the H109 $\alpha$  velocity of 2.4 km sec<sup>-1</sup>. At present no reliable distance for RCW38 is available; however, from its longitude of about 270° it probably lies in the Orion arm. Wilson *et al.* (1970) have suggested that the distance is between 0.5 and 1.5 kpc, as for RCW36. Goss, Murray, and Radhakrishnan (1970) find a lower limit of 2 kpc from 21 cm absorption measurements.

The broad absorption line in RCW38 is not nearly as favourable as that in W12 for Zeeman-splitting measurements. A series of observations of the Stokes parameter *V* gave a peak-to-peak noise of 0.5 degK for an integration time of 2.4 hr with 10 kHz bandwidth.

*(f) G282.0-1.2*

The galactic radio source G282.0-1.2 is an HII region which has an H109 $\alpha$  recombination line velocity of 23 km sec<sup>-1</sup>; this implies a position beyond the solar

circle with a kinematic distance of 7 kpc. Weak absorption at 1665 MHz was found by McGee, Gardner, and Robinson (1967).

The four ground-state OH profiles with 10 kHz resolution are shown in Figure 7(a). Absorption is present at 1612, 1665, and 1667 MHz. The properties of these three lines are summarized in Table 4 and the line ratios are given in Table 5.

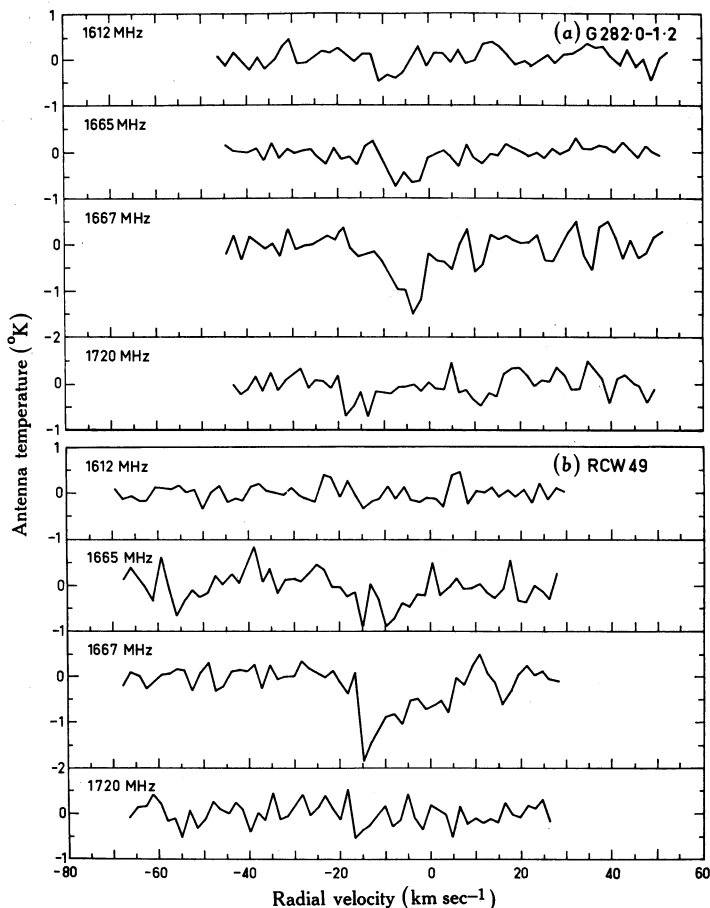


Fig. 7.—OH profiles, recorded with 10 kHz bandwidth, for (a) G282.0-1.2 and (b) G284.3-0.3 (RCW 49).

(g) G284.2-0.8

The strong emission from this source has been discussed previously (Manchester, Goss, and Robinson 1969*a*, 1969*b*), but complete profiles at all frequencies have not been previously published. As discussed in the previous papers, the OH emission position is between the two continuum sources G284.0-0.9 (RCW 48) and G284.3-0.3 (RCW 49). The position is given on the 5000 MHz continuum map of Goss and Shaver (1970) in Figure 8, showing that the emission is apparently associated with the extended thermal source G284.0-0.9. However, the association is not certain and it is possible that it is one of projection only.

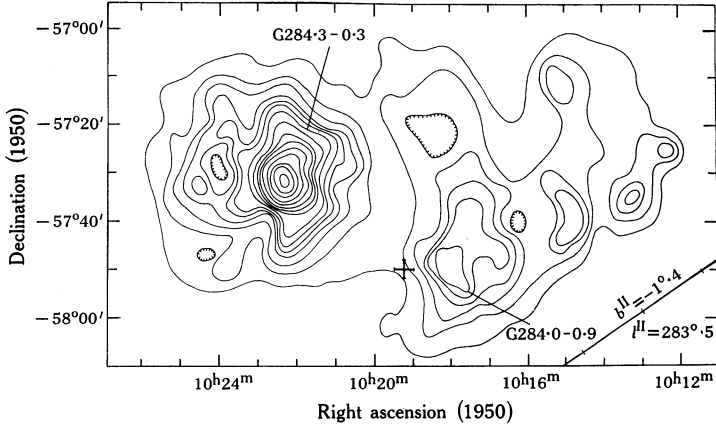


Fig. 8.—Map of the region near  $l^{II} = 284^\circ$  at 6 cm wavelength (Goss and Shaver 1970) with a  $4'$  arc beam. The cross marks the position of the OH emitter G284.2-0.8; the size of the cross indicates the errors in the position.

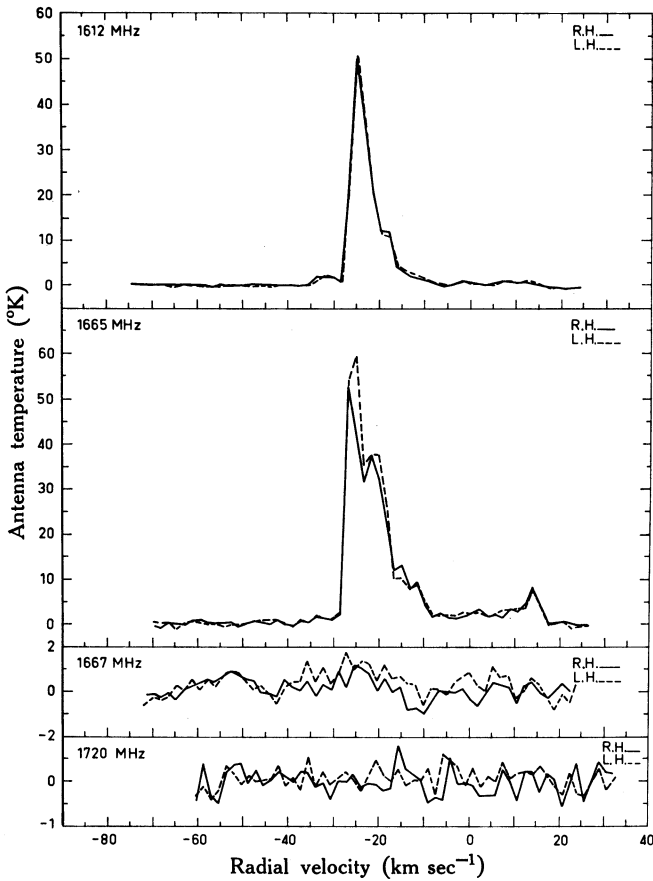


Fig. 9.—OH profiles of G284.2-0.8 taken with a bandwidth of 10 kHz.

Observations with 10 kHz resolution at the continuum maximum of G284.0-0.9 do not show absorption at any frequency. At 1667 MHz any absorption is less than  $0.5^\circ\text{K}$ , corresponding to a limiting optical depth of about 0.03.

Profiles taken with 10 kHz resolution at the emission position R.A.  $10^{\text{h}} 19^{\text{m}} 42^{\text{s}}$ , Dec.  $-57^\circ 50' 1$  are shown in Figure 9. At both 1612 and 1665 MHz there is strong emission between  $-29$  and  $-15$  km sec $^{-1}$  and weaker but significant emission between  $-15$  and  $+17$  km sec $^{-1}$ . In addition there is 1612 MHz emission between  $-29$  and  $-35$  km sec $^{-1}$  which has no counterpart at 1665 MHz. Within the positioning errors the strong 1612 and 1665 MHz emission, and the weaker 1665 MHz emission at 14 km sec $^{-1}$ , all arise from the same position. The 1667 and 1720 MHz profiles show that there is no significant emission at these frequencies. There may be weak 1667 MHz absorption near  $-10$  km sec $^{-1}$ .

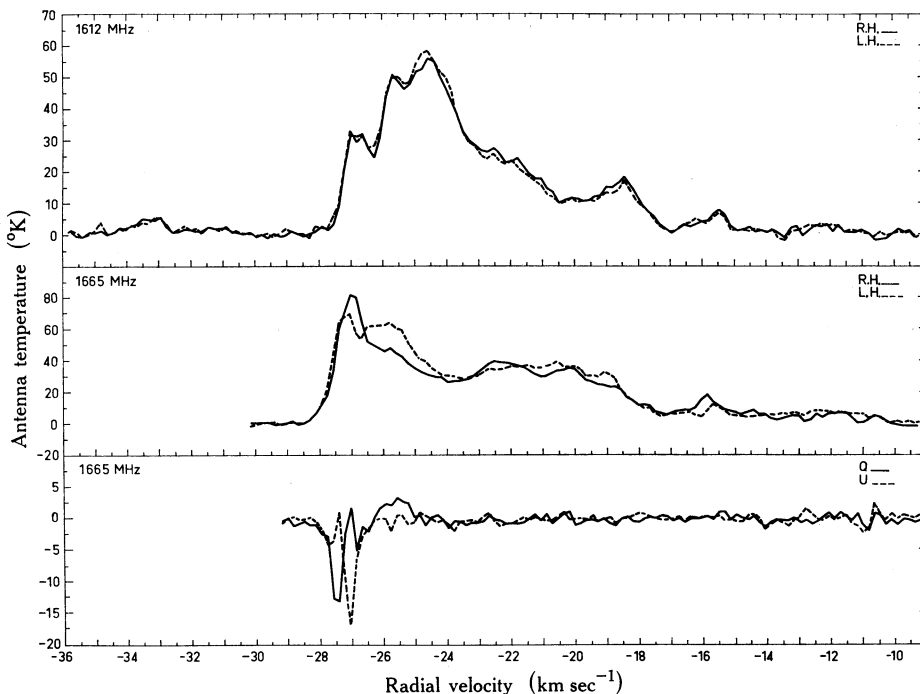


Fig. 10.—Polarization of part of the OH emission from G284.2-0.8 at 1612 and 1665 MHz. The bandwidth is 1 kHz.

Figure 10 shows profiles of the more intense portion of the 1612 and 1665 MHz emission, taken with 1 kHz resolution. The 1612 MHz emission is unpolarized at all velocities, the limits for the stronger emission around  $-24.5$  km sec $^{-1}$  being  $< 4\%$  circular and  $< 2\%$  linear polarization. At 1665 MHz most of the emission is unpolarized, but there are several polarized features at the low-velocity end. As shown in Table 3, these features have both linear and circular polarization. The unpolarized component has a peak flux density of 106 f.u. at  $-27.2$  km sec $^{-1}$ .

The emission from this source has a number of unusual characteristics. At both 1612 and 1665 MHz the emission covers a very wide velocity range ( $-35$  to  $+17$  km sec $^{-1}$ ) and is intense. The profiles have little fine structure or narrow band emission and little or no polarized component. Although the emission shows a general similarity at the two frequencies, there is no detailed correspondence. The 1612 MHz emission is unusually strong compared to that from most other sources which emit strongly at 1665 MHz, and the lack of any absorption or emission at 1667 MHz is also notable. Most OH emission sources (except those associated with infrared stars) have been found close to a continuum radio source, but G284.2—0.8 is in a region of weak continuum emission. Few similar cases would have been observed in the searches for OH emission sources, which have recorded the profiles at the peak of continuum sources; few systematic observations have been made at other positions.

No kinematic distance can be given for the OH emission source owing to the wide velocity range covered. As discussed by Manchester, Goss, and Robinson (1969*a*), photometric observations indicate that G284.0—0.9 may be at a distance of approximately 4 kpc. Measurements discussed below indicate that G284.3—0.3 is at a distance of about 6 kpc. However, the emission from G284.2—0.8 may not be associated with either of these continuum sources.

(*h*) G284.3—0.3

The intense continuum source G284.3—0.3 is the HII region RCW 49. OH absorption at 1665 MHz was discovered by McGee, Gardner, and Robinson (1967). The H109 $\alpha$  recombination line velocity is  $-0.1$  km sec $^{-1}$ . The choice of the far distance (5 kpc) for RCW 49 by Manchester, Goss, and Robinson (1969*a*) is based on the appearance of an OH absorption line at  $-13.1$  km sec $^{-1}$ . This velocity is close to the tangential velocity and hence the near distance can be excluded. The far distance has been confirmed by recent 21 cm absorption measurements by Radhakrishnan (personal communication). Westerlund (1960) considers that a distance of 6 kpc is most likely for RCW 49.

The OH profiles for RCW 49 are shown in Figure 7(*b*) (10 kHz resolution); only the 1665 and 1667 MHz profiles show detectable absorption. The properties of the 1667 MHz absorption lines are summarized in Table 4. The measured optical depth is an order of magnitude less than for the stronger absorption sources.

(*i*) G285.2—0.0

Emission at 1665 MHz has been observed from the small thermal source G285.3—0.0, which is situated about  $1^\circ$  east of the strong continuum source G284.3—0.3 (RCW 49). Figure 11(*a*) shows profiles with 10 kHz resolution taken on all four frequencies at the continuum maximum of G285.3—0.0 (R.A.  $10^{\text{h}} 29^{\text{m}} 48^{\text{s}}$ , Dec.  $-57^\circ 46' .7$ ). At 1665 MHz there is R.H. circular emission at velocities near 4 and 9 km sec $^{-1}$  and L.H. circular emission at about 6 km sec $^{-1}$ .

This emission comes from a position near the continuum maximum of G285.3—0.0 at R.A.  $10^{\text{h}} 29^{\text{m}} 31^{\text{s}} \pm 16^{\text{s}}$ , Dec.  $-57^\circ 45' .3 \pm 2'$ . This position is marked on the map of the 5000 MHz continuum emission in Figure 12. There is no absorption apparent at any velocity or frequency, the limiting value for the optical depth at 1667 MHz being 0.04.

Figure 11(b) shows profiles with 1 kHz resolution taken at the 1665 MHz emission position. The 1665 MHz profiles show that the L.H. and R.H. circular features are independent and each is 100% polarized. Details of the polarization of these emission features are given in Table 3. No emission is evident in Figure 11(b) on the other three frequencies.

The H109 $\alpha$  recombination line velocity is  $-1.0 \text{ km sec}^{-1}$ . This velocity is relatively close to the velocities of OH emission and suggests that G285.3-0.0 is close to the solar circle at a distance of 5.3 kpc. A plate taken at Mt. Stromlo on the Uppsala Schmidt camera by Dr. G. Lyngå (personal communication) shows a small dense emission region at the position of G285.2-0.0 to the west of the Carina Nebula.

(j) *Carina Nebula*

The Carina Nebula is a complex of HII regions near  $l^{\text{II}} = 288^\circ$  (Beard and Kerr 1966), whose distance has been determined by several optical investigations; the mean value is 2.7 kpc (Sher 1965a). Absorption at 1667 MHz was first detected by McGee, Gardner, and Robinson (1967).

The four ground-state OH profiles taken with 10 kHz resolution for the continuum source G287.5-0.6 are shown in Figure 13. Absorption lines are seen at 1665 and 1667 MHz and their properties are summarized in Tables 4 and 5. The optical depths are an order of magnitude less than in the stronger absorption sources. The velocity of the OH absorption line is within  $2 \text{ km sec}^{-1}$  of one of the H109 $\alpha$  recombination lines in the Carina Nebula (Gardner *et al.* 1970).

(k) *G291.3-0.7*

The 5 GHz continuum map of the area of RCW 57 is shown in Figure 14. It includes the continuum source G291.3-0.7, a compact thermal source (NGC 3576) with an emission measure of greater than  $10^7 \text{ cm}^{-6} \text{ pc}$  (Shaver and Goss 1970). Strong absorption of this source has been observed on all four OH lines. Figure 15 shows profiles taken at the 18 cm continuum maximum position (R.A.  $11^{\text{h}} 09^{\text{m}} 50^{\text{s}}$ , Dec.  $-61^\circ 01' 7''$ ) with 10 kHz resolution. The absorption profile is of the same form at each of the four frequencies and consists of a narrow line centred at  $-25.8 \text{ km sec}^{-1}$  with a weaker absorption feature on the high velocity side. Line ratios for the absorption given in Table 5 show that the level populations are not consistent with a unique excitation temperature. If the absorbing OH were assumed to cover only a portion of the source, the 1667:1665 MHz line ratio indicates that the optical depth would be very large (16.7) with a filling factor of about 0.16. On the other hand, the 1667:1720 MHz line ratio is actually greater than the theoretical value for small optical depth.

Observations of the 1667 MHz absorption have been made at a grid of points on G291.3-0.7 and the adjacent source G291.6-0.5 (NGC 3603), as marked by the small crosses in Figure 14. The optical depth of the  $-25.8 \text{ km sec}^{-1}$  absorption may be slightly larger on the western points but generally shows little variation over the square grid on G291.3-0.7 with a mean value of about 0.15. Absorption at this velocity is also present on the two eastern points; for the point at R.A.  $11^{\text{h}} 11^{\text{m}} 30^{\text{s}}$  the optical depth is about 0.04, and for the point at R.A.  $11^{\text{h}} 12^{\text{m}} 20^{\text{s}}$  it is about 0.015. Thus the absorbing OH at  $-25.8 \text{ km sec}^{-1}$  extends in front of G291.6-0.5.

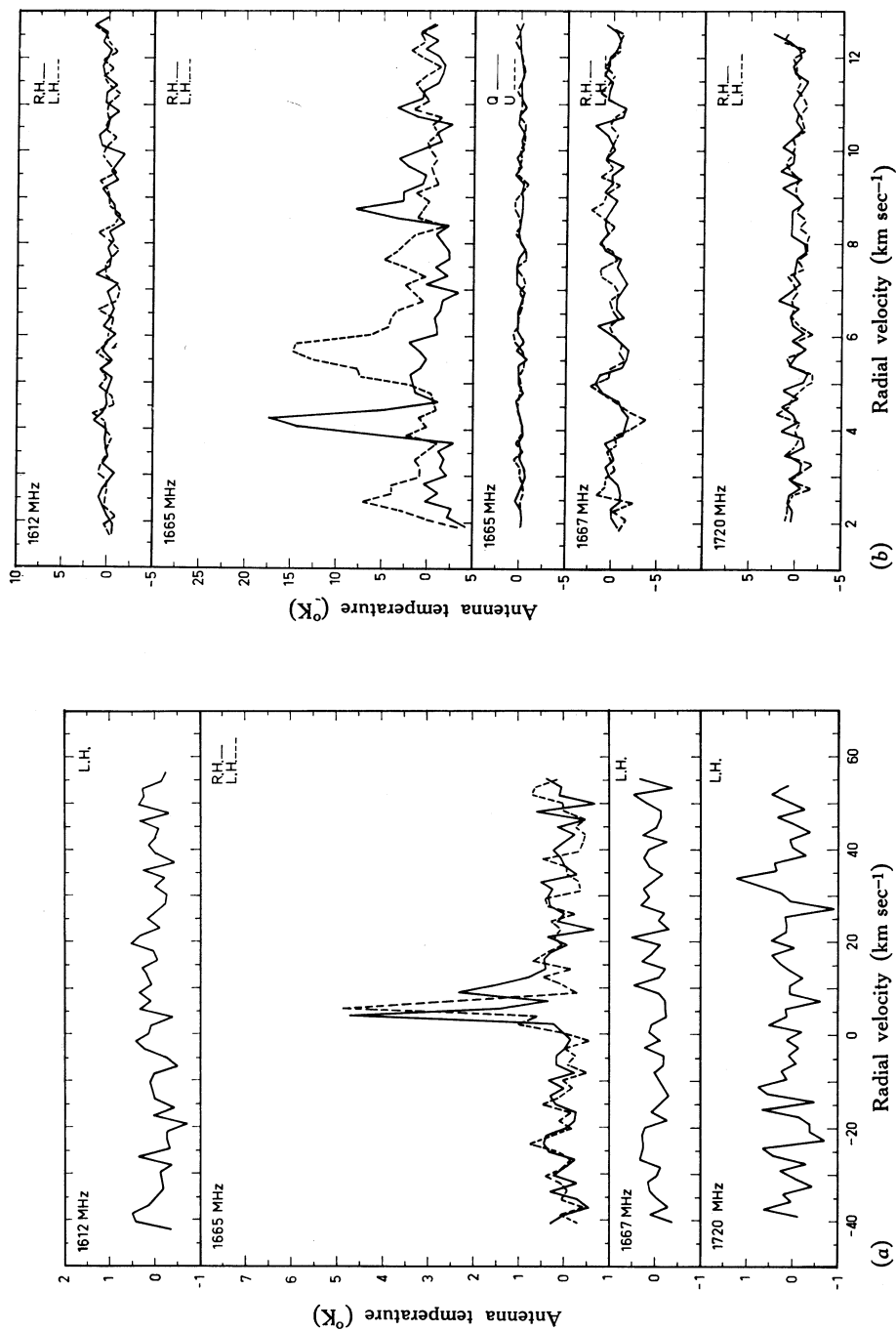


Fig. 11.—OH profiles taken at (a) the position of the continuum maximum in G285.3-0.0 (R.A. 10<sup>h</sup> 29<sup>m</sup> 48<sup>s</sup>, Dec. -57° 46'.7), the bandwidth being 10 kHz, and (b) the position of the 1665 MHz emission from G285.2-0.0 (R.A. 10<sup>h</sup> 29<sup>m</sup> 31<sup>s</sup>, Dec. -57° 45'.3), the bandwidth being 1 kHz.

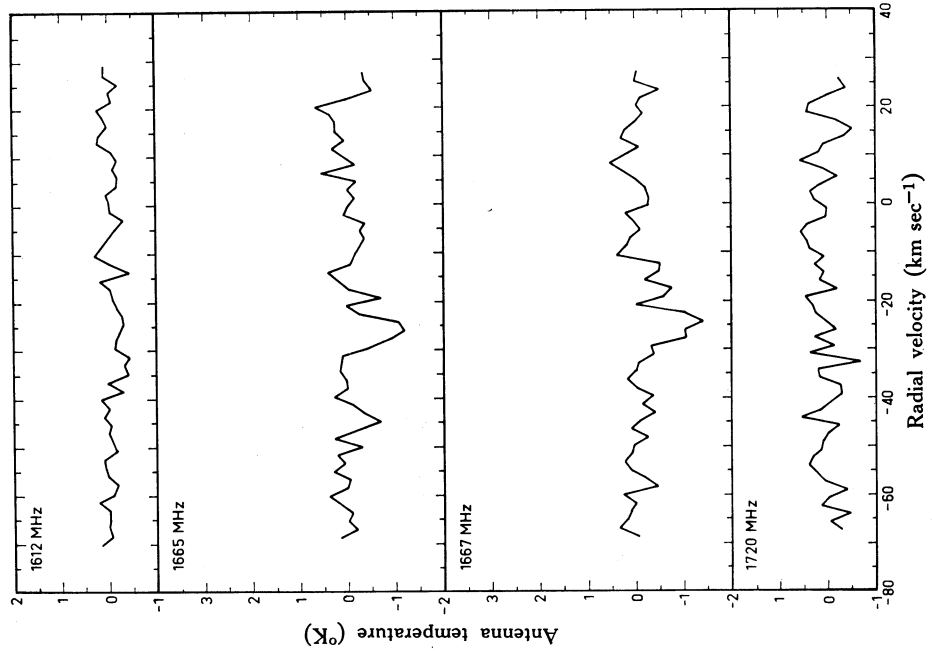


Fig. 12 (*above*).—Map of G285.3-0.0 at 6 cm wavelength (Goss and Shaver 1970) with a 4' arc beam. The cross marks the position of the 1665 MHz emitter G285.2-0.0; the size of the cross indicates the errors in the position.

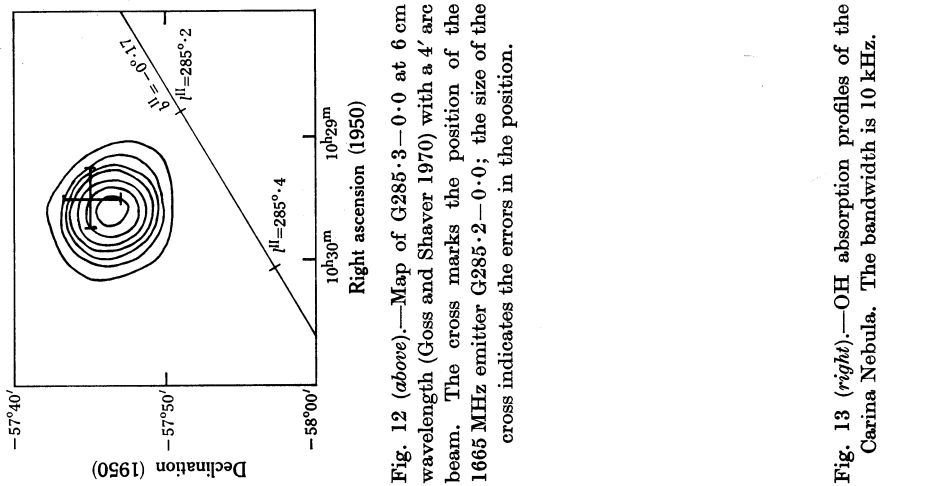


Fig. 13 (*right*).—OH absorption profiles of the Carina Nebula. The bandwidth is 10 kHz.

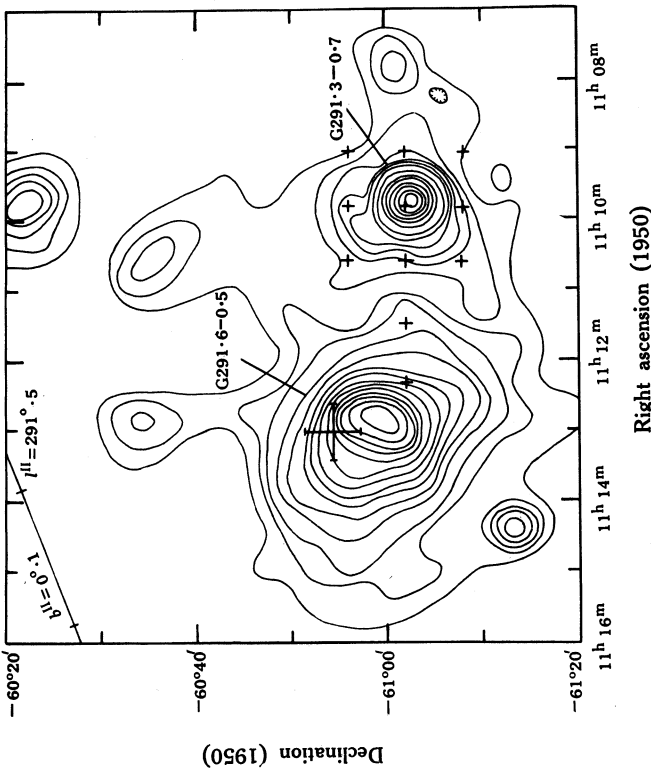
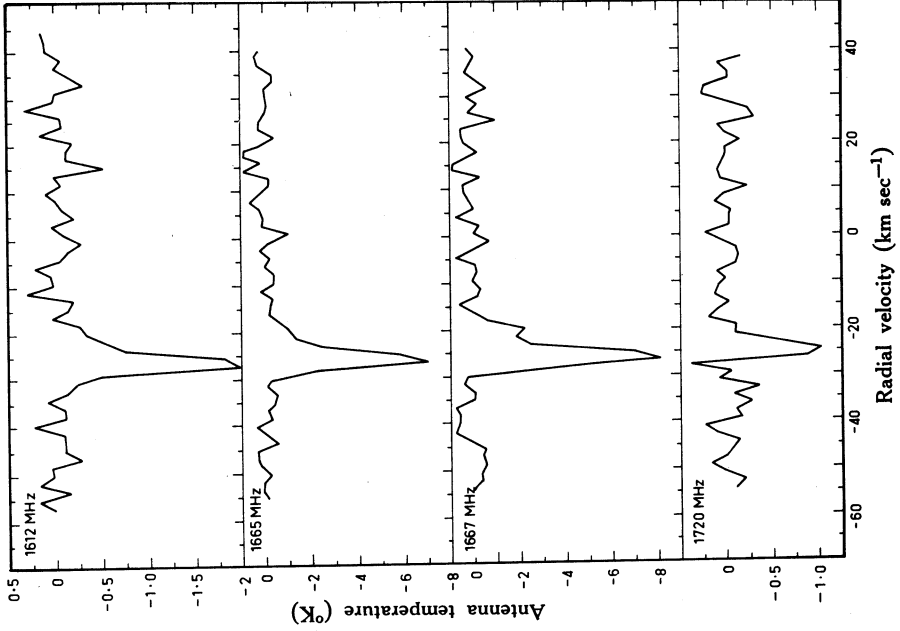


Fig. 14 (above).—Map of the region near  $l_{II} = 291.5$  at 6 cm wavelength (Goss and Shaver 1970) with a 4' arc beam. The small crosses show the grid over which OH absorption profiles were measured. The large cross marks the position of the OH emission from G291.6-0.4; the size of the cross indicates the errors in the position.

Fig. 15 (right).—OH absorption profiles for G291.3-0.7. The bandwidth is 10 kHz.

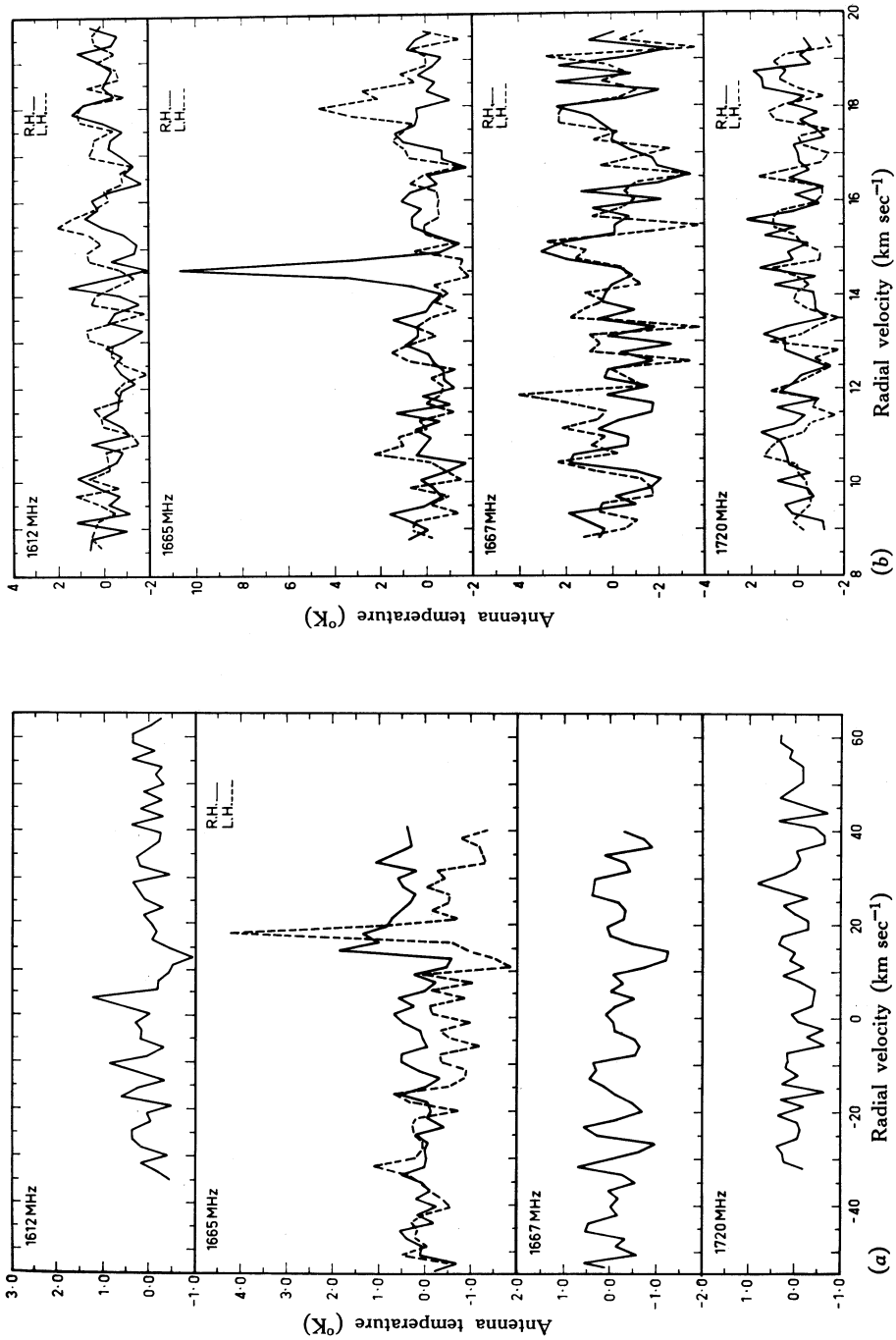


Fig. 16.—OH profiles taken at (a) the continuum maximum of G291.6-0.5 (R.A. 11<sup>h</sup> 13<sup>m</sup> 15<sup>s</sup>, Dec. -60° 58'.5), the bandwidth being 10 kHz, and (b) the position of the 1665 MHz emission from G291.6-0.4 (R.A. 11<sup>h</sup> 13<sup>m</sup> 00<sup>s</sup>, Dec. -60° 54'.5), the bandwidth being 1 kHz. The profiles at 1612, 1667, and 1720 MHz in (a) are averages of measurements with L.H. and R.H. circular polarization.

As discussed below, there is weak absorption with optical depth 0.013 at  $+13.1 \text{ km sec}^{-1}$  on the continuum maximum of G291.6-0.5. This absorption is also present on the two eastern grid points discussed above, but there is no evidence for absorption at this velocity at the continuum maximum of G291.3-0.7, with a limiting optical depth of 0.01. These measurements suggest that G291.6-0.5 and the absorbing OH at  $+13.1 \text{ km sec}^{-1}$  are both more distant than G291.3-0.7. They also show that the absorbing OH at  $-25.8 \text{ km sec}^{-1}$  extends only about 20' arc to the east of the G291.3-0.7 position.

The H109 $\alpha$  recombination line velocity for G291.3-0.7 is  $-22.8 \text{ km sec}^{-1}$ , close to the OH absorption velocity. This velocity indicates a position near the tangential point of galactic rotation at a distance of about 3.6 kpc. Observations of hydrogen line absorption (Goss and Radhakrishnan 1969) also show that G291.3-0.7 is at or beyond the tangential point.

The absorption line in G291.3-0.7 is similar in width to that in RCW 38, and so is not very suitable for Zeeman-splitting measurements. Observations of the Stokes parameter  $V$  at 1665 MHz gave a peak-to-peak noise of 1.0 degK for an integration time of 2.9 hr with 10 kHz bandwidth.

(l) G291.6-0.4

OH has been observed in emission at 1665 MHz and in absorption at 1612, 1665, and 1667 MHz for the thermal source G291.6-0.5. This source is associated with the nebula NGC 3603. On the 5 GHz continuum map of the region in Figure 14, G291.6-0.5 is seen to be extended.

In Figure 16(a) profiles taken with 10 kHz resolution are reproduced for the four OH frequencies at the continuum maximum position, R.A.  $11^{\text{h}} 13^{\text{m}} 15^{\text{s}}$ , Dec.  $-60^{\circ} 58' .5$ . These show evidence for a weak absorption line at about  $+13 \text{ km sec}^{-1}$  at 1612, 1665, and 1667 MHz. The distribution of this absorption (as measured at 1667 MHz) has been discussed in Section IV(k).

Emission at 1665 MHz appears to rise from the high-velocity side of the absorption, making the absorption parameters given in Table 4 for this frequency very approximate. The emission originates at a position (R.A.  $11^{\text{h}} 13^{\text{m}} 00^{\text{s}} \pm 24^{\text{s}}$ , Dec.  $-60^{\circ} 54' .5 \pm 3'$ ) on the northern side of the continuum source, as marked in Figure 14. Profiles taken at this position with 1 kHz resolution are given in Figure 16(b). The L.H. and R.H. circular emission features at 1665 MHz are independent and well separated in velocity. As shown in Table 3, they are both 100% circularly polarized, within the noise, and have no significant linear component.

The kinematic distance of G291.6-0.5 corresponding to the H109 $\alpha$  recombination line velocity of  $+10.4 \text{ km sec}^{-1}$  is beyond the solar circle at approximately 8.4 kpc. This is the only possible kinematic distance. Sher (1965b) has determined a distance of 3.5 kpc for the compact cluster at the centre of NGC 3603 using photometric observations. Observations of hydrogen line absorption (Goss and Radhakrishnan 1969) show that G291.6-0.5 is beyond the tangential point, so the kinematic distance given above is adopted. The OH absorption velocity of  $+13.1 \text{ km sec}^{-1}$  is slightly greater than the recombination line velocity, but the velocity difference is well within the range found for most cases of absorption near HII regions (see Section V(a)).

## V. CHARACTERISTICS OF OH IN SOUTHERN SOURCES

We shall now summarize some of the main characteristics of OH absorption and emission associated with sources in the longitude range  $128^\circ$ – $50^\circ$ , as covered here and in the two companion papers (Robinson, Goss, and Manchester 1970; Goss, Manchester, and Robinson 1970).

## (a) Absorption

Strong absorption on all four 18 cm OH lines is seen in the continuum sources W 12, RCW 38, G291.3–0.7, Sgr A, Sgr B2, and W 43. Much weaker absorption is observed in RCW 46, RCW 49, and the Carina Nebula. In no cases do the relative intensities of the absorption on the four 18 cm lines correspond to those expected in thermal equilibrium. In particular, the absorption on 1612 MHz is always different from that on 1720 MHz, although these two lines have approximately equal transition probabilities. The absorption at 1720 MHz is stronger in W 12, RCW 36, and RCW 38, similar to the case of M 17 (Goss 1968); the 1612 MHz absorption is stronger in RCW 46, G291.3–0.7, and W 43, similar to that in W 22 and Cas A (Goss 1968).

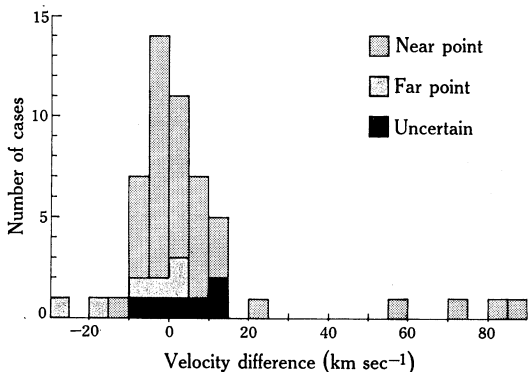


Fig. 17.—Histogram showing the difference between the H109 $\alpha$  recombination line velocity (Wilson *et al.* 1970) and the OH absorption velocity for both northern and southern sources. For sources with  $90^\circ < l^{\text{II}} < 180^\circ$  and  $270^\circ < l^{\text{II}} < 360^\circ$  the sign of the velocity difference has been reversed.

Comparison of OH absorption radial velocities and the corresponding hydrogen recombination line velocities from Wilson *et al.* (1970) shows that in many cases the absorbing OH and the HII region are closely related. The histogram in Figure 17 shows the difference between the recombination line velocity and OH absorption velocity for all HII regions discussed in the three papers of this series, and also those HII regions discussed by Goss (1968) and Weaver, Dieter, and Williams (1968) but not included in these papers. For sources in the quadrants  $l^{\text{II}} = 90^\circ$ – $180^\circ$  and  $270^\circ$ – $360^\circ$  the sign of the velocity difference has been reversed. Therefore, except when the continuum source is beyond the tangential point of galactic rotation, the absorption (being closer) should give a positive velocity difference. Sources which are beyond the tangential point and those whose distance is ambiguous have been indicated in the figure. Except for those sources beyond the tangential point, only one negative velocity difference greater than  $10 \text{ km sec}^{-1}$  is observed. Although in many cases the line of sight to the source passes through or along spiral-arm regions, the diagram shows that in most cases the absorbing OH and the HII region are closely associated; 75% of the velocity differences are less than  $10 \text{ km sec}^{-1}$ . It would appear that conditions favourable for the formation of OH (and other molecules) are also favourable for star formation and subsequent generation of HII regions.

*(b) Emission on Satellite Lines*

The 1720 MHz line appears in emission, with the other three lines in absorption, in Sgr A, W 28, W 44, and W 43B, as discussed by Goss (1968) and Goss and Robinson (1968). This type of emission was first noted in Cas A by Rogers and Barrett (1967). The first three sources are nonthermal while W 43B is a thermal source with an  $H109\alpha$  velocity close to the 1720 MHz emission velocity. In all cases the emission profile is broad and has a low degree of polarization. In W 28, W 43B, and W 44 the optical depth of the absorption on 1667 MHz is higher (typically by a factor of two) at the position of the 1720 MHz emission than at the continuum maximum. This suggests that the OH density reaches a maximum near the location of the 1720 MHz emission. The angular size of the emission in W 28 has been found by scintillation observations to be greater than  $1''$  arc. This is much greater than the sizes found for the most common class of source emitting at 1665 MHz, for which the angular sizes are between  $0''.005$  and  $0''.1$ .

Weak emission at 1612 MHz, with absorption on the other three lines, is observed in RCW 38 and probably in RCW 36. This emission also has a low degree of polarization. Much stronger 1612 MHz emission, perhaps associated with weak 1665 MHz emission, is found in W 43A near radial velocities of 27 and 40  $\text{km sec}^{-1}$ . The lines are wide and at 40  $\text{km sec}^{-1}$  there is slight elliptical polarization. The 1612 MHz emission from W 43A has some similarities to that from the infrared object CIT -3, in which broad emission features with low polarization occur at two widely separated velocities, and there is only weak main line emission.

*(c) New Types of OH Emission*

Intense 1612 MHz emission, with weaker main line emission, occurs in G331.5-0.1 (Robinson, Goss, and Manchester 1969). This case differs from that of CIT -3 and W 43A by having a number of sharp emission spikes near one velocity, with a high degree of circular polarization.

Strong emission at 1612 and 1665 MHz has been found in G284.2-0.8 (Manchester, Goss, and Robinson 1969a, 1969b). For each line the emission covers a very wide velocity range, with no polarization at 1612 MHz and only a few elliptically polarized features at 1665 MHz. The line emission comes from a region of weak continuum emission adjacent to the thermal source G284.0-0.9.

In G24.3+0.1 emission occurs only at 1667 MHz, as originally observed by Goss (1968). Wide emission lines are present at two well-separated velocities, and in each case there is 100% *linear* polarization.

*(d) Main Line Emission associated with HII Regions*

Of the thermal sources investigated in the range  $128^\circ \leq l^{\text{III}} \leq 50^\circ$  there are 14 cases of strong main line emission. The agreement of the OH and hydrogen recombination line velocities (see Table 6) shows that the emitting OH is in close proximity to the HII region. The velocities in Table 6 refer to the emission sources covered by the present series of papers, and also northern sources from the papers by Weaver, Dieter, and Williams (1968), Ellder, Rönning, and Winnberg (1969), Rydbeck, Ellder, and Kollberg (1969), Turner (1969), and Downes (1970). Except

for the cases of NGC 6334B and W 43C, the strongest emission is at 1665 MHz. The lines are narrow and have a high degree of circular or elliptical polarization; in the latter case the profiles for the linear Stokes parameters  $Q$  and  $U$  have very narrow features which are unresolved by the 1 kHz filters, although the circular polarization profiles are adequately resolved (e.g. G305.4+0.2, NGC 6334A, NGC 6334B, W 33A).

TABLE 6

COMPARISON OF RADIAL VELOCITIES FOR OH EMISSION AND HYDROGEN RECOMBINATION LINE

Galactic Source Number	Previous Designation	H109 $\alpha$ Radial Velocity (km sec <sup>-1</sup> )	Velocity Range for OH Emission at 1665 and 1667 MHz (km sec <sup>-1</sup> )	$V_{109\alpha} - \bar{V}_{OH}$ (km sec <sup>-1</sup> )
G0.7-0.0	Sgr B2	62.0	+54 to +74.5	-5
G5.9-0.4	—	10.5	-35 to +30	+31
G10.6-0.4	—	0.3	-2.4 to -0.3	+3
G12.7-0.2	W 33B	35.8*	+59 to +66	(-26)
G12.9-0.3	W 33A	35.8*	+36 to +41	-4
G20.0-0.2	—	43.4	+45.5 to +47.5	-3
G30.6-0.1	W 43C	44†	+35 to +38	(+7)
G43.2+0.0	W 49	9.0	+1 to +24	-7
G49.5-0.4	W 51	58.5	+57 to +62	0
G70.3+1.6	NGC 6857	-24.4	-21.4 to -19.7	-3
G75.8+0.4	—	-4.8	-6 to +3	-4
G81.7+0.6	W 75A	1.7‡	-1 to +6	+1
G81.9+0.7	W 75B	1.7‡	+3 to +13	-6
G111.5+0.8	NGC 7538	-60.6	-59.8 to -59.4	-1
G133.9+1.1	W 3	-43.5	-50 to -41	+2
G209.0-19.4	Orion A	-2.2	-6 to +24	-10
G285.2-0.0	—	-1.0	+2 to +11	-6
G291.6-0.4	NGC 3603	+10.4	+14 to +19	-4
G305.4+0.2	1308-62	-38.5	-40 to -33	-2
G331.5-0.1	1608-51	-88.1	-93 to -86	+2
G333.2-0.5	1617-50	-55.2	-56 to -48	-4
G333.6-0.2	1618-49	-47.7	-53 to -47	+3
G351.1+0.7	NGC 6334B	-2.6	-15 to -3.5	+7
G351.4+0.7	NGC 6334A	-2.6	-13 to -7	+8

\* H109 $\alpha$  velocity of G12.8-0.2.

† Location of recombination line is not known. G30.8-0.0 has an H109 $\alpha$  velocity of 92.7 km sec<sup>-1</sup>.

‡ H109 $\alpha$  velocity of DR 23.

The main line emission is accompanied by emission on both satellite lines in 3 of the 14 sources; in another 3 there is emission at 1612 MHz only and 1 case with 1720 MHz emission only, while in the remaining 7 cases there is no detectable satellite emission. The 1612 or 1720 MHz emission is always circularly polarized.

Temporal variations over periods of several months have been seen at 1665 MHz in NGC 6334A, NGC 6334B, and W 33A, and at 1720 MHz in W 49 and W 51. No variations have been seen with a time scale as short as a few days, but observations are lacking for time scales between a week and several months.

## (e) Zeeman Splitting of Absorption Lines

No polarization has been detected in any of the absorption profiles. A search has been made for Zeeman splitting of the deep absorption of W12 at 1665 and 1667 MHz, and an upper limit of  $5 \times 10^{-5}$  G can be set for the longitudinal magnetic field in the absorbing OH cloud(s). For HI clouds various authors (e.g. Verschuur 1970) have suggested that the magnetic field is frozen in and so is amplified as the cloud condenses. If, as is generally believed, the absorbing OH exists in clouds which have contracted to greater densities, the W12 result suggests that field amplification has not continued.

## VI. ACKNOWLEDGMENTS

The receivers used were designed, installed, and operated by Mr. M. W. Sinclair, who also gave valuable assistance with the observations. The computer programs were developed by Mr. D. J. Smart. One of us (W.M.G.) acknowledges the support of a N.A.T.O. Postdoctoral Fellowship during part of this work.

## VII. REFERENCES

- BEARD, M., and KERR, F. J. (1966).—*Aust. J. Phys.* **19**, 875.  
 CLARK, B. G., RADHAKRISHNAN, V., and WILSON, R. W. (1962).—*Astrophys. J.* **135**, 151.  
 DOWNES, D. (1970).—*Astrophys. Lett.* **5**, 53.  
 ELLDER, J., RÖNNÄNG, B., and WINNBERG, A. (1969).—*Nature, Lond.* **222**, 67.  
 GARDNER, F. F., MILNE, D. K., MEZGER, P. G., and WILSON, T. L. (1970).—The Carina Nebula at 6 cm. *Astr. Astrophys.* (in press).  
 GOSS, W. M. (1968).—*Astrophys. J. Suppl. Ser.* **15**, 131.  
 GOSS, W. M., MANCHESTER, R. N., and ROBINSON, B. J. (1970).—*Aust. J. Phys.* **23**, 559.  
 GOSS, W. M., MURRAY, J. D., and RADHAKRISHNAN, V. (1970).—*Proc. astr. Soc. Aust.* **1**, 332.  
 GOSS, W. M., and RADHAKRISHNAN, V. (1969).—*Astrophys. Lett.* **4**, 199.  
 GOSS, W. M., and ROBINSON, B. J. (1968).—*Astrophys. Lett.* **2**, 81.  
 GOSS, W. M., and SHAVER, P. A. (1970).—*Aust. J. Phys. astrophys. Suppl.* No. 14, 1.  
 HILL, E. R. (1968).—*Aust. J. Phys.* **21**, 735.  
 MCGEE, R. X., GARDNER, F. F., and ROBINSON, B. J. (1967).—*Aust. J. Phys.* **20**, 407.  
 MCGEE, R. X., ROBINSON, B. J., GARDNER, F. F., and BOLTON, J. G. (1965).—*Nature, Lond.* **208**, 1193.  
 MANCHESTER, B. A., and GOSS, W. M. (1969).—*Aust. J. Phys. astrophys. Suppl.* No. 11, 35.  
 MANCHESTER, R. N., GOSS, W. M., and ROBINSON, B. J. (1969a).—*Astrophys. Lett.* **3**, 11.  
 MANCHESTER, R. N., GOSS, W. M., and ROBINSON, B. J. (1969b).—*Proc. astr. Soc. Aust.* **1**, 212.  
 PALMER, P., and ZUCKERMAN, B. (1967).—*Astrophys. J.* **148**, 727.  
 RAIMOND, E., and ELIASSON, B. (1969).—*Astrophys. J.* **155**, 817.  
 ROBINSON, B. J., GOSS, W. M., and MANCHESTER, R. N. (1969).—*Proc. astr. Soc. Aust.* **1**, 211.  
 ROBINSON, B. J., GOSS, W. M., and MANCHESTER, R. N. (1970).—*Aust. J. Phys.* **23**, 363.  
 RODGERS, A. W., CAMPBELL, C. T., and WHITEOAK, J. B. (1960).—*Mon. Not. R. astr. Soc.* **121**, 103.  
 ROGERS, A. E. E., and BARRETT, A. H. (1967).—*Proc. I.A.U. Symp.* No. 31, p. 77.  
 RYDBECK, O. E. H., ELLDER, J., and KOLLBERG, E. (1969).—*Astrophys. J. Lett.* **156**, 141.  
 SHAVER, P. A., and GOSS, W. M. (1970).—*Aust. J. Phys. astrophys. Suppl.* No. 14, 133.  
 SHER, D. (1965a).—*Q. Jl. R. astr. Soc.* **6**, 299.  
 SHER, D. (1965b).—*Mon. Not. R. astr. Soc.* **129**, 237.  
 TURNER, B. E. (1969).—*Astrophys. J.* **157**, 103.  
 VERSCHUUR, G. L. (1970).—Magnetic fields in the Galaxy. *Proc. I.A.U. Symp.* No. 38 (in press).  
 WEAVER, H. F., DIETER, N. H., and WILLIAMS, D. R. W. (1968).—*Astrophys. J. Suppl. Ser.* **16**, 219.  
 WESTERLUND, B. (1960).—*Ark. Astr.* **2**, 419.  
 WILSON, W. J., and BARRETT, A. H. (1968).—*Science, N.Y.* **161**, 778.  
 WILSON, T. L., MEZGER, P. G., GARDNER, F. F., and MILNE, D. K. (1970).—*Astr. Astrophys.* **6**, 364.

